$NiFe_2O_4$-CNT Composite: An Efficient Electrocatalyst for Oxygen Evolution Reactions in Li-O_2 Batteries Guided by Computations

Xin Zhang, Xu Zhang, Xin-Gai Wang, Zhaojun Xie,* Zhen Zhou*

Tianjin Key Laboratory of Metal and Molecule Based Material Chemistry, Institute of New Energy Material Chemistry, Collaborative Innovation Center of Chemical Science and Engineering (Tianjin), School of Materials Science and Engineering, National Institute for Advanced Materials, Nankai University, Tianjin 300350, P.R. China. Email: zjxie@nankai.edu.cn(ZX); zhouzhen@nankai.edu.cn (ZZ)

Computational Methods

First-principles calculations based on density functional theory (DFT) were performed by using the plane-wave technique as implemented in the Vienna ab initio simulation package (VASP).[1] The projector augmented wave (PAW) pseudopotential was adopted.[2] A 500 eV cutoff was used for the plane wave basis set. Considering the strong electron correlation effects, all calculations involving Fe and Ni atoms were performed at the DFT+U level with a U value of 3.3 and 5.5 eV, respectively.[3] The Perdew, Burke, and Ernzerhof (PBE) functional of generalized gradient approximation (GGA) was used for calculating the exchange-correlation energy.[4] The Brillouin zone was represented by Monkhorst-Pack special *k*-point meshes of 6×4×1 for $NiFe_2O_4/Li_2O_2$ and 11×5×1 for Li_2O_2. The model was an orthogonal supercell as shown in Fig. S1 (a). In the $NiFe_2O_4/Li_2O_2$ system, the $Li_2O_2(0001)$ surface located on $NiFe_2O_4$ (111) surface is shown in Fig. 1 (b). The lattice mismatch is ≈3 %. To avoid any artificial interactions between the periodically repeated images along c axis, a vacuum space of at least 18 Å was inserted.

The standard free energy of Li_2O_2 is calculated by:

$$\Delta G_f^\circ = G_{Li_2O_2(s)}^\circ - 2G_{Li(s)}^\circ - G_{O_2(g)}^\circ$$
$$= \Delta E_f + \Delta E_{zpe} - T\Delta S$$

where ΔE_f is the formation energy of Li_2O_2, ΔE_{zpe} is the zero point energy correction and ΔS is the entropy of O_2 under standard conditions (T = 298 K). According to the Nernst Equation, $U_0 = -\Delta G_f^\circ/ne$, the calculated open-circuit potential of $2Li^+ + O_2 \leftrightarrow Li_2O_2$ is 3.00 V, which is very close to the experimental value (2.96 V). The slight error might be caused by the inaccuracy of DFT in estimating the cohesive energy of O_2.[5, 6] However, since the same cohesive energy value of O_2 was used to estimate the formation of Li_2O_2 in this work, the calculated free energy is comparable at the same standard and the predicted tendency is reliable. The atomic charge was calculated by means of Bader's charge population analysis.[7, 8]

In order to understand the charging process, the free energy change of each step was described as the following equation:

$$\Delta G(m) = \Delta E_{tot}(m) + \Delta E_{zpe}(m) - T\Delta S(m) - eU$$

where m represents the corresponding reaction step (m = 1, 2, 3), $\Delta E_{tot}(m)$, $\Delta E_{zpe}(m)$ and $\Delta S(m)$ are the change of total energy, zero point vibrational energy and entropy under standard conditions (T = 298K) in step m, respectively.[6, 9] U is the electromotive force corresponding to the charging voltage which was calculated by $\Delta G = \Delta G_f^\circ + nUF$. F is Faraday's constant. In this work, the overpotential was defined by shifting the free energy of all intermediates to $\Delta G \leq 0$, which is consistent with the previous research.[10, 11] For the computations of pure

Li_2O_2, the lower two layers atoms were fixed and for $Li_2O_2/NiFe_2O_4$ systems, the lower two layers atoms of $NiFe_2O_4$ and the upper two layers of Li_2O_2 were fixed. Other atoms were fully relaxed.

Details on the calculation of ΔG_f°

The standard free energy of Li_2O_2 is calculated by:

$$\Delta G_f^\circ = G_{Li_2O_2(s)}^\circ - 2G_{Li(s)}^\circ - G_{O_2(g)}^\circ \quad (1)$$

$$G_{Li_2O_2(s)}^\circ = E_{f[Li_2O_2(s)]} + E_{zpe[Li_2O_2(s)]} - T\Delta S_{Li_2O_2(s)}(T) \quad (2)$$

$$G_{Li(s)}^\circ = E_{f[Li(s)]} + E_{zpe[Li(s)]} - T\Delta S_{Li(s)}(T) \quad (3)$$

$$G_{O_2(g)}^\circ = E_{f[O_2(g)]} + E_{zpe[O_2(g)]} - T\Delta S_{O_2(g)}(T) \quad (4)$$

The following equation can be obtained from (1), (2), (3) and (4).

$$\Delta G_f^\circ = E_{f[Li_2O_2(s) - 2Li(s) - O_2(g)]} + E_{zpe[Li_2O_2(s) - 2Li(s) - O_2(g)]} - T\Delta S_{[Li_2O_2(s) - 2Li(s) - O_2(g)]}(T) \quad (5)$$

Moreover, the entropy changes of Li_2O_2(s) and Li(s) can be neglected, thus equation (5) can be written as:

$$\Delta G_f^\circ = \Delta E_f + \Delta E_{zpe} - T\Delta S(T) \quad (6)$$

The entropy of O_2 at standard condition (298 K) can be taken from NIST database, which is 205.138 J K^{-1} mol^{-1}, thus the calculated entropy change for O_2 is 0.63 eV at 298 K. On the basis of the results, the formation Gibbs free energy for Li_2O_2 can be calculated (-6.00 eV) which is consistent with experimental values.[12-14]

Material Preparation

All the reagents were the analytical grade without further purification. CNTs were purchased from J&K. In the synthesis process, 0.175 g $Ni(NO_3)_2 \cdot 6H_2O$, 0.485 g $Fe(NO_3)_3 \cdot 9H_2O$, and 0.45 g urea were dissolved in 30 ml of distilled water and ethanol mixture (1:4 volume ration) where ~1.5 mg ml^{-1} of CNTs were added. The suspension was sonicated for 30 min in a bath sonicator, and then heated at 180 ^oC for 12h in a 50 ml Teflon-lined stainless steel autoclave. After cooling, the precipitate, i.e. $NiFe_2O_4$-CNTs, were washed thoroughly with the distilled water and ethanol, and dried at 120 ^oC in a vacuum oven. $NiFe_2O_4$ was also prepared according to the above-mentioned steps without adding CNTs.

Materials Characterizations

Field emission scanning electron microscope (FESEM) images were obtained on a JEOL-JSM 7500 microscope. The energy dispersive X-ray spectroscopy (EDS) attached to the SEM instrument was used to analyze the material. High Resolution transmission electron microscope (HRTEM) graphs were taken on a FEI Tecnai G2F20 field emission TEM. X-ray Diffraction (XRD) was performed to characterize the discharge and charge products on a D/MAX III diffractometer with Cu Kα radiation. X-ray photoelectron spectroscopy (XPS) was performed on Axis Ultra DLD (Kratos Analytical). N_2 adsorption/desorption isotherms were obtained by using ASAP 2020/Tristar 3000 Surface Area and Pore Size Analyzer.

Battery assembles and electrochemical Tests

The cathodes were prepared as follows. $NiFe_2O_4$-CNT and polyvinylidenefluoride (PVDF) were mixed under magnetic agitation at a weight ratio of 9:1 with N-methyl-2-pyrrolidinone (NMP) as the solvent at room

temperature. The mixture was then sprayed homogeneously onto one side of the circular carbon paper (ϕ12 mm) and dried in an oven at 80°C overnight. As the comparison, the CNT cathodes were made through the same procedure. The electrochemical performances were evaluated in Swagelok-type cells with a 1.0 cm^2 hole in the cathode, enabling O_2 to flow in. The batteries were assembled in a glove box filled with high-purity argon (O_2 and H_2O < 1 ppm). The batteries composed of lithium metal anodes, ploytetrafluoroethylene (PTFE) separators, and $NiFe_2O_4$-CNT or CNT cathodes. The electrolyte composed of 1M lithium bis(trifluoromethanesulfonyl)imide (LiTFSI) dissolved in tetraethylene glycol dimethyl ether (TEGDEM). Electrochemical measurements were performed on the LAND-CT2001A tester at room temperature. Galvanostatic discharge-charge measurements were conducted within a voltage range of 2-4.3 V. Cycling performances were recorded at a current density of 200 mA g^{-1} with a cutoff capacity of 1000 mAh g^{-1}. We conducted cyclic voltammetry (CV) on a CHI600C electrochemical workstation between 2.0-4.5 V with a sweep rate of 0.1 mV s^{-1} in oxygen atmosphere.

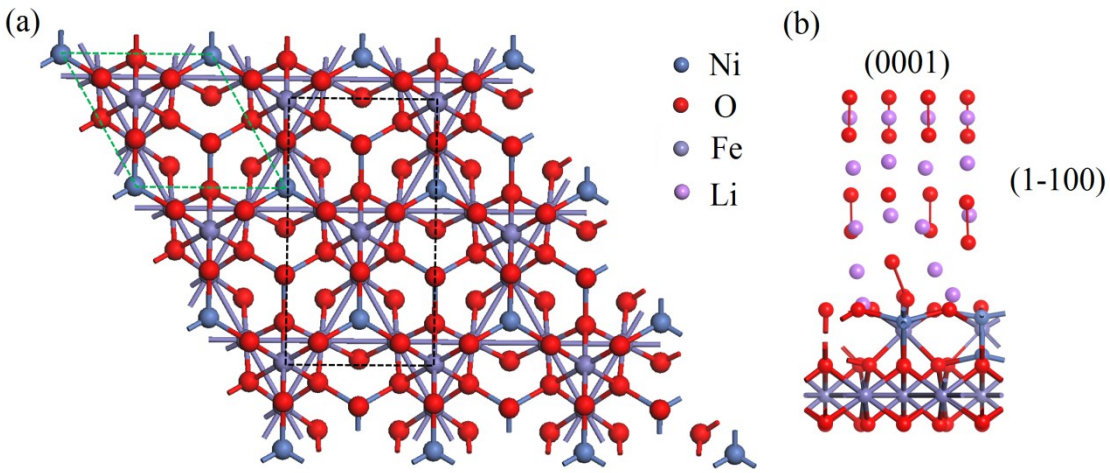

Fig. S1 (a) Geometry of $NiFe_2O_4$ (111) surface. The area circulated by green lines represents the hexagonal primitive cell and circulated by black lines represent the orthogonal supercell. (b) The side view of the $NiFe_2O_4/Li_2O_2$ system.

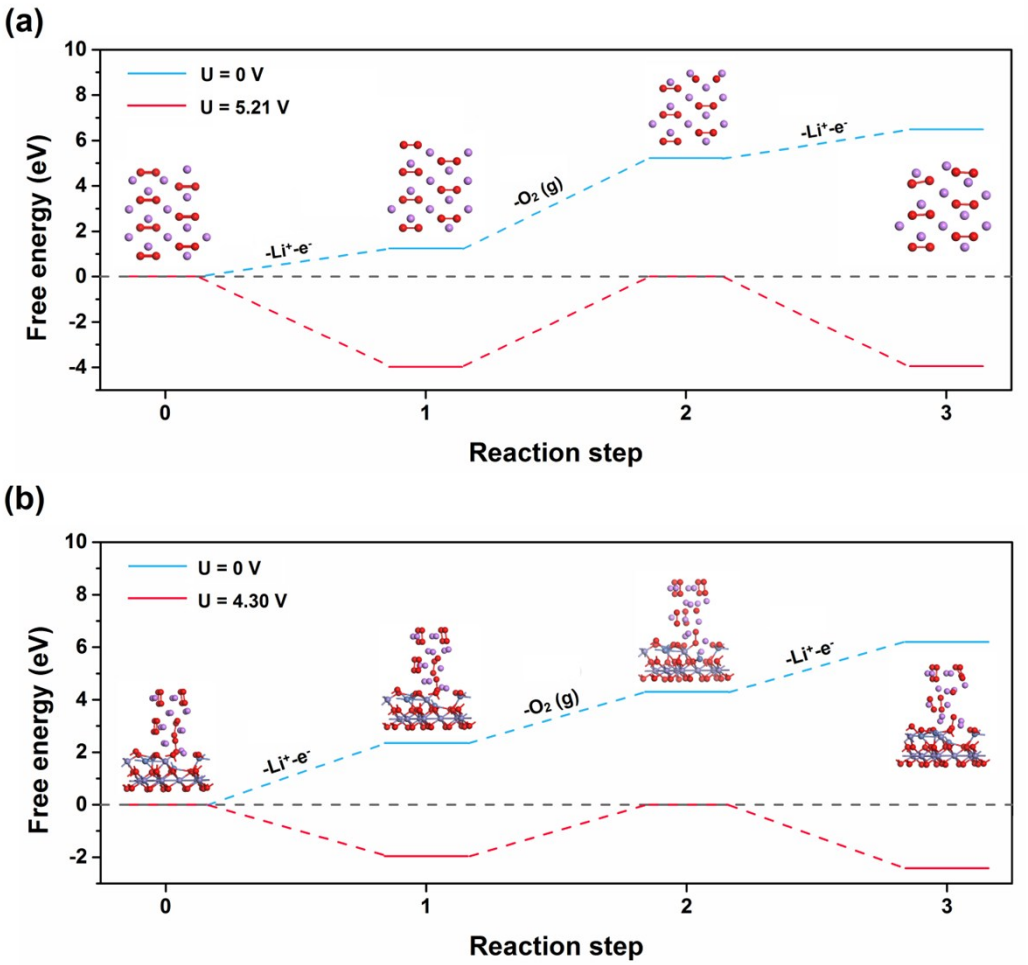

Fig. S2 Calculated energetic profiles of the OER for Li_2O_2 (a) and Li_2O_2 deposited on $NiFe_2O_4$ (b) for path II. The blue and red lines are under the potential of U = 0 V and U= 5.21 V (a), 4.30 V (b), respectively.

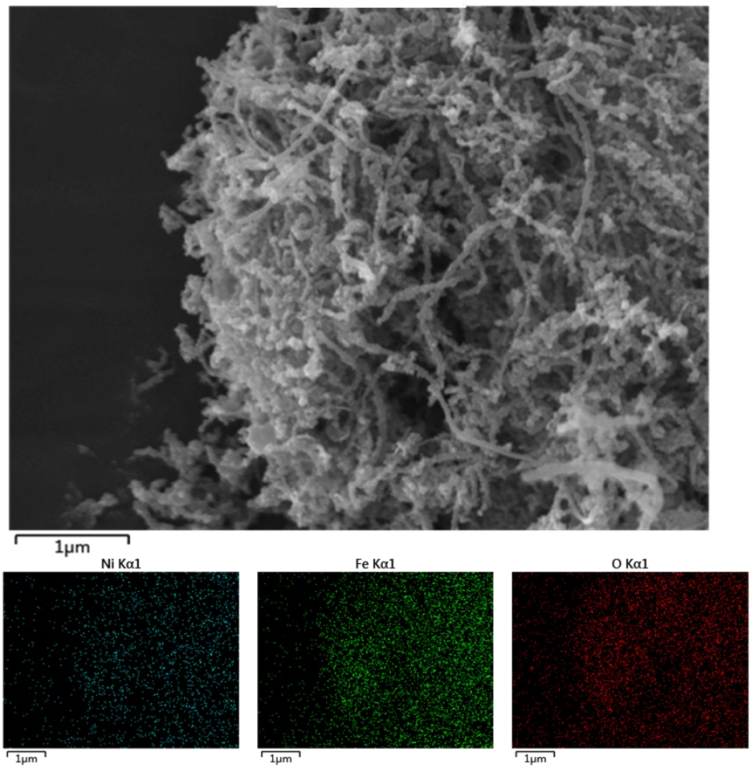

Fig. S3 Elemental mappings showing uniformly distributed Ni, Fe, and O elements in $NiFe_2O_4$-CNT composite.

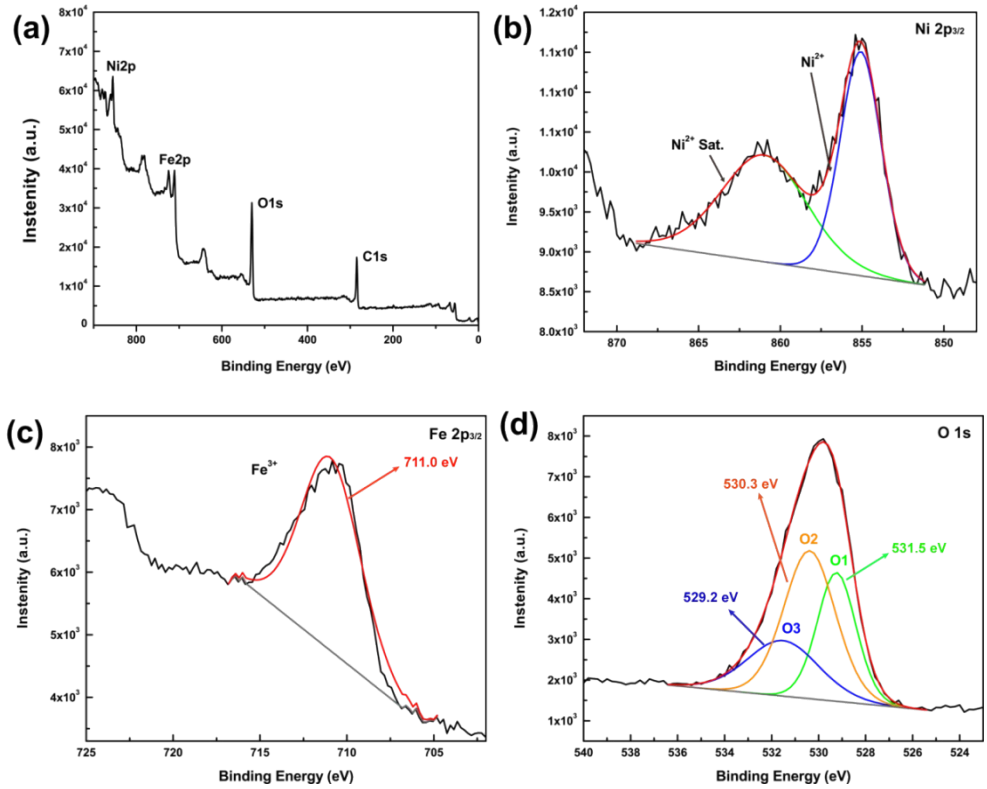

Fig. S4 (a) XPS survey spectrum of $NiFe_2O_4$-CNT composite. High-resolution XPS spectra of (b) Ni $2p_{3/2,}$ (c) Fe $2p_{3/2}$ and (d) O 1s.

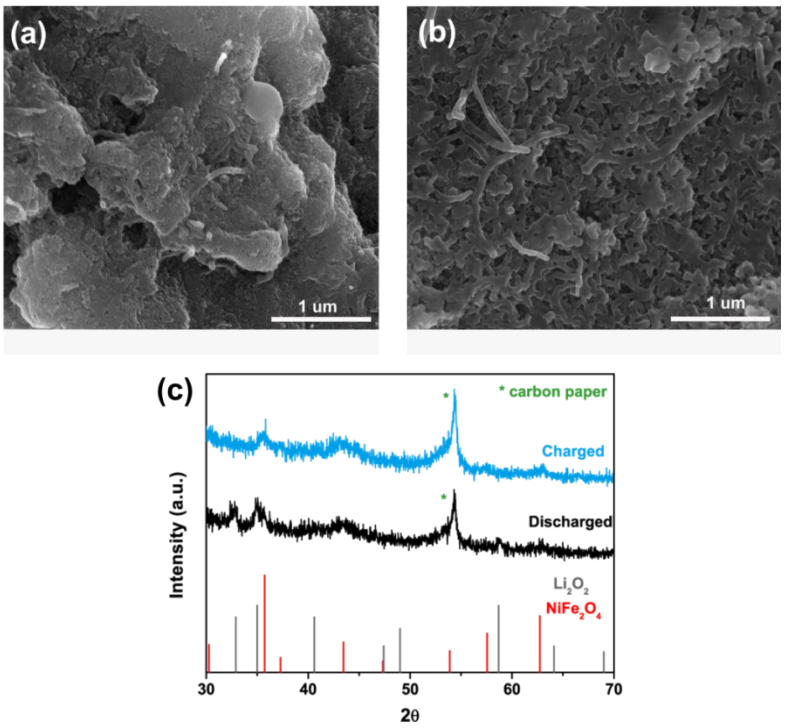

Fig. S5 SEM images (a and b) and (c) XRD patterns of the cathodes at discharged and charged state.

1. G. Kresse and J. Furthmüller, Phys. Rev. B, 1996, 54, 11169.
2. G. Kresse and D. Joubert, Phys. Rev. B, 1999, 59, 1758.
3. Y.-F. Li and A. Selloni, ACS Catal., 2014, 4, 1148-1153.
4. J. P. Perdew, K. Burke and M. Ernzerhof, Phys. Rev. Lett., 1996, 77, 3865.
5. J. S. Hummelshoj, J. Blomqvist, S. Datta, T. Vegge, J. Rossmeisl, K. S. Thygesen, A. C. Luntz, K. W. Jacobsen and J. K. Norskov, J. Chem. Phys., 2010, 132, 071101.
6. Y. Jing and Z. Zhou, ACS Catal., 2015, 5, 4309-4317.
7. G. Henkelman, A. Arnaldsson and H. Jónsson, Comp. Mater. Sci., 2006, 36, 354-360.
8. E. Sanville, S. D. Kenny, R. Smith and G. Henkelman, J. Comput. Chem., 2007, 28, 899-908.
9. Y. Hwang, K.-H. Yun and Y.-C. Chung, J. Power Sources, 2015, 275, 32-37.
10. Y. Mo, S. P. Ong and G. Ceder, Phys. Rev. B, 2011, 84, 2054461.
11. J. Zhu, X. Ren, J. Liu, W. Zhang and Z. Wen, ACS Catal., 2015, 5, 73-81.
12. Y. Xu and W. A. Shelton, J. Electrochem. Soc., 2011, 158, A1177-A1184.
13. Y. Xu and W. A. Shelton, J. Chem. Phys., 2010, 133, 024703.
14. J. S. Hummelshøj, J. Blomqvist, S. Datta, T. Vegge, J. Rossmeisl, K. S. Thygesen, A. Luntz, K. W. Jacobsen and J. K. Nørskov, J. Chem. Phys., 2010, 132, 071101.